Chapter

Measuring the Blind Holes: Three-Dimensional Imaging of through Silicon via Using High Aspect Ratio AFM Probe

Imtisal Akhtar, Malik Abdul Rehman and Yongho Seo

Abstract

Three-dimensional integration and stacking of semiconductor devices with high density, its compactness, miniaturization and vertical 3D stacking of nanoscale devices highlighted many challenging problems in the 3D parameter's such as CD (critical dimension) measurement, depth measurement of via holes, internal morphology of through silicon via (TSV), etc. Current challenge in the high-density 3D semiconductor devices is to measure the depth of through silicon via (TSV) without destructing the sample; TSVs are used in 3D stacking devices to connect the wafers stacked vertically to reduce the wiring delay, power dissipation, and of course, the form factor in the integration system. Special probes and algorithms have been designed to measure 3D parameters like wall roughness, sidewall angle, but these are only limited to deep trench-like structures and cannot be applied to structures like via holes and protrusions. To address these problems, we have proposed an algorithm based nondestructive 3D Atomic Force Microscopy (AFM). Using the high aspect ratio (5, 10, 20, 25) multiwall carbon nanotubes (MWCNTs) AFM probe, the depth of holes up to 1 micron is faithfully obtained. In addition to this, internal topography, side walls, and location of via holes are obtained faithfully. This atomic force microscopy technique enables to 3D scan the features (of any shape) present above and below the surface.

Keywords: algorithms, AFM, surface characterization, carbon nanotube, 3D AFM, sidewall, through silicon via (TSV)

1. Introduction

Scanning probe microscopy (SPM) over the former 20 years has been intensively used by many research groups due to its applicability in extensive filed of materials. In past 50 years, the most significant advancement in AFM was ranked at second place [1–8]. This is because the application of AFM not limited to the semiconductor field but also covers many wide range fields like chemical group identification [9], cell biological [10], semiconductor to study the properties of the materials at nanoscale [11]. Although, applications and techniques of SPM are diverse in nature, but they do share a common feature, i.e., probe to sense localized or confined signal, because in many cases the probe that confines the spatial accuracy.

AFM [12] is the most common form of SPM in which the probe is usually in the form of sharp, rigid and having long-life time mounted on the cantilever or tuning fork to transduce the tip-sample force. However, depending upon the application of AFM probe, it might have different shapes, length but the constant geometry over a long-time is common thing in all types of probes. As the probe scanning over the sample, the topography of the surface is constructed depending upon the mode of operation of AFM. The ensued image depicts the geometry of tip corresponding to the surface geometry.

Noteworthy improvement and advancement in the instrumentation, correction of artifacts and scanning algorithms has been accomplished. In addition to this, different type of probes has been prepared to obtain the deep trench (DT) [13] and sidewall roughness (SWR) [14], tracing vertical sidewalls [15], overhang and undercut features [16], etc. In addition to this, many useful techniques such as reflectometry [17] to measure the depth of via holes, X-Ray methods [18] and atomic force microscopy (AFM). Each method has its own pros and cons. For examples, conventional AFM is unable to image the features having high aspect ratio such a silicon pillars or deep via holes. In addition to this, reflectometry is also a useful and non-destructive technique. However, its resolution is limited to optical microscopy. Moreover, in some of the measurement instruments prior knowledge of sample surface is required.

In silicon industry, many improvements in the instrumentation has been done to measure the dimensions up to several hundred nanometer scale [19], lithography, manipulation of individual etc. In nanotechnology, AFM always is the essential contrivance especially when it comes to the height measurement of the feature. Because, measuring the deep, narrow via holes always been difficult and mainly unsolved problem. Measuring the depth of the hole is not enough and situation become worse and complicated when the sidewalls of the hole needs to be scanned. Many other groups also tried to increase the functionality and versatility of AFM either by combining the optical instrument [20] with atomic force microscopy but that is just limited to scan the trench to smaller dimension or limited to visible spectrum. In addition to this, flair shape probe [21], trident probe [22], bi-pod, capped probe [23], Osborne [22], hammerhead [24] and many other shaped probes are designed to address problem related to scanning. However, there is not one-size-fit-all answer. Seo et al. [25] has proposed general algorithm for scanning the deep via holes. However, that general algorithm has not been implemented on samples. One of the major problem associated with the algorithm was it does not stored the motion of probe when it find the sidewall wall in either direction which is necessary to keep following the boundary of the sample. Also, in case of no wall around, the tip moved one step further along the previous direction of motion. In this case, at some point, tip will lost the boundary of sample.

In this work we methodically explorer the scanning algorithm to scan the different types of features present above (protrusion) or below (holes) the surface and removed the problem associated with [24]. We have used the single MWCNT as a scanning probe attached by dielectrophoresis and FIB treatment. In addition to this, first time we have successfully implemented the non-destructive technique with high aspect ratio on real samples to obtain the three-dimension topography, depth measurement of holes, position of via holes by force-distance mapping for not only holes as well as protrusion.

2. Experimental method

There are mainly two aspects of fabrication of quartz tuning fork sensor followed by ball capped nanotube: nanotube attachment on electrochemically

etched tungsten probe and modification using FIB treatment. In the complete process several steps are involved as shown in **Figure 1**. The tuning fork sensor is characterized by the length of carbon nanotube attached, radius of the ball capped on the top of MWCNT and orientation (angle with respect to the surface). All these parameters define the resolution, severity and image appearances of the tip.

2.1 Fabrication of tungsten tips

A 85% potassium hydroxide (KOH) was purchased from Sigma Aldrich® Company. A 2 molar concentration of KOH aqueous solution was prepared by dissolving KOH pallets in deionized water. After that, solution was agitated thoroughly to make it homogenous and left for 1 h. A gold wire with 200 μm diameter and 10 mm length was used as cathode. Tungsten (W) wire with diameter 50 and 25 mm length, with 99.95% purity, was purchased from Alfa Aesar® and used as anode. To improve the crystallinity, rapid thermal annealing (RTA) was done at 800°C for 40 s. DC voltages (typically 3–5 volts) are applied between gold and Tungsten

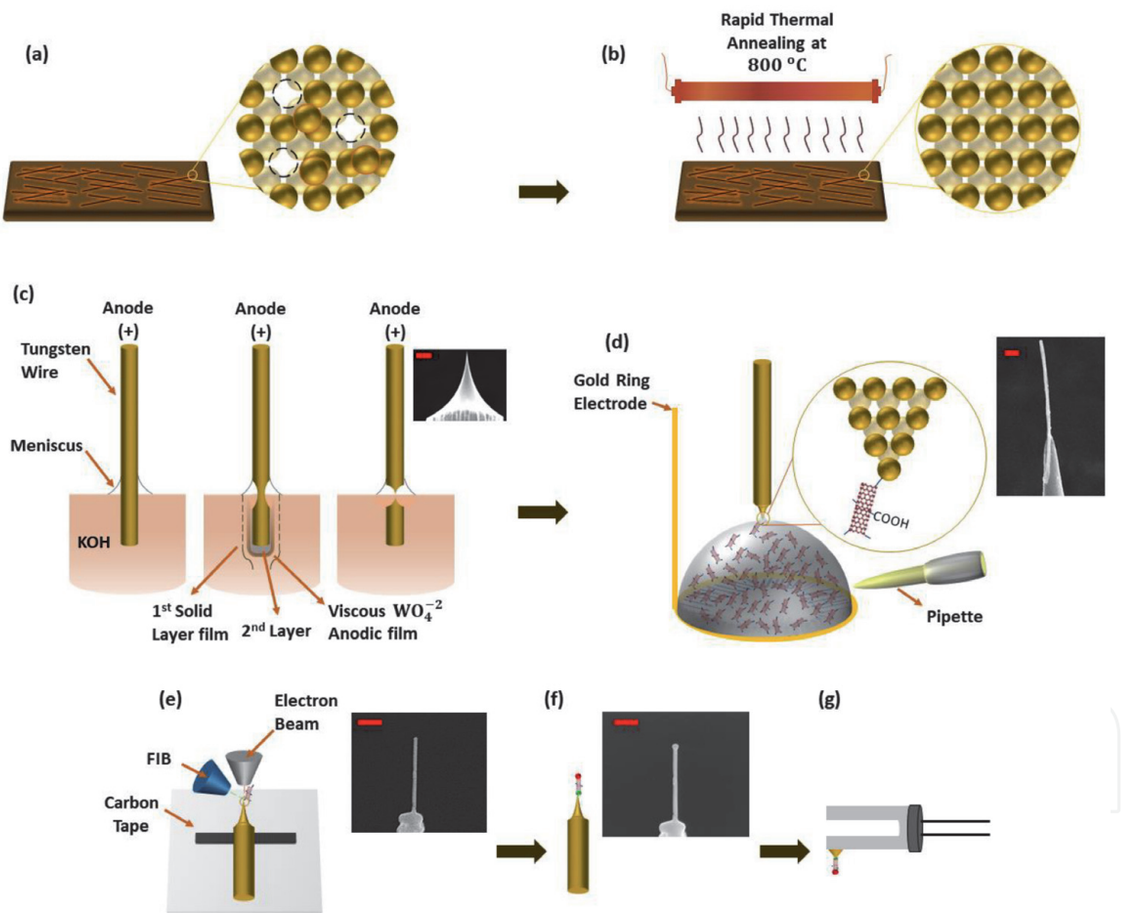

Figure 1.
Fabrication of tuning fork sensor followed by ball capped nanotube (a) Tungsten wire was annealed at 800°C *for 40 s to improve the crystallinity. (b) Crystallinity of tungsten wire has been improved as the atoms are arranged at the lattice points. (c) Electrochemical etching using KOH produce very sharp tip of the order 65 nm. This diameter is ideal to attach all three types of CNTs (110–170 nm, 50–80 nm, 20 nm). (d) Small droplet of functionalized MWCNTTs is picked using micropipette and poured on gold ring electrode. Using Micromanipulator tip brings closer to droplet and meniscus is formed which covers the edge part of tungsten probe. AC voltages are applied across the electrodes (gold electrode and tungsten probe). SEM image of CNT attached at the apex of tungsten probe. Scale bar is 500 nm. (e) Tungsten probe followed by MWCNT is fixed on substrate using carbon tape and cutting, welding and capping was done using FIB. Carbon is deposited at the junction of MWCNT and tungsten so that it is firmly attached (welded) with tungsten. For stability purpose, excess length of CNT is cut-off. Gallium ions are used to cut the excess length of CNT. (f) Carbon atoms are deposited on the top of CNT to form a ball-capped shape to make it suitable for scanning of via holes. (g) Attachment of FIB treated tungsten probe with the quartz tuning fork.*

electrodes using 2 M KOH aqueous solution. Keithley 32,220 function generator is used to apply DC voltage across the electrodes. By applying the DC voltage, redox reaction occurs at the electrodes and tungsten tip begins to narrow. The shape of the neck depends upon the meniscus formed at the air-liquid interface. The experimental setup for electrochemical etching is shown in **Figure A3**. Reaction takes place can be described by the following equation [26].

At anode

$$6H_2O + 6e^- \rightarrow 3H_2(g) + 6OH^-$$

At cathode

$$W(s) + 8OH^- \rightarrow WO_4^{2-} + 4H_2O + 6e^-$$

Overall, reaction can be summarized as:

$$W(s) + 2OH^- + 2H_2O \rightarrow WO_4^{2-} + 3H_2\,(g) \quad (1)$$

The hydrogen gas bubbles produced during the etching should be avoided as it disturbs the meniscus which affects the shape of probe. Due to this, glass slide is placed between the electrodes. During the etching process, variation in the thickness of tungsten wire and current was monitored using the CCD camera and oscilloscope. When the current drops below the set point, shut-off circuit trigger the solid state relay (shut-off time is 0.5 ns), sharp edge of the tungsten wire is formed and hence in this way over-etching does not happen. The home-built automatic cutoff circuit to avoid over-etching is used as shown in **Figure A1**. After the wire has been etched, it was washed with the hot distilled water (D.I) to reduce the oxide layer around the edge and examined under the scanning electron microscope. Tips with the sharp edges are reserved for next step (attachment of MWCNT with tungsten probe) as these are the best candidates used for D.E.P.

2.2 Functionalization and multiwall carbon nanotubes attachment with tungsten tip using dielectrophoresis

We have used commercially available MWCNTs (Sigma Aldrich). First two MWCNTs samples having 110–170 nm (10 μm in length) and 60 nm (15 μm in length) diameter are grown by chemical vapor deposition (CVD) and 20 nm (30 μm in length) diameter MWCNTs was grown by arc discharge method. The reason why we used the un-purified carbon nanotubes is to reveal that anyone can easily make the carbon nanotubes tips in one's laboratory, because MWCNTs made by arc discharge are very difficult to purify. To obtain a single MWCNT, fictionalization of MWCNTs is good choice. Other than that, it is difficult to attach single MWCNT on tungsten tip. Firstly, to functionalize the MWCNTs (with different diameter as 100–170 nm, 60 nm, 20 nm), 1 g of PVA was completely dissolved in 60 ml of water at room temperature. After that, 0.2 mg of MWCNTs was added in to the above-mentioned solution and mixture was stirred at 70°C for four 12 h. Secondly, centrifugation machine was used to remove the impurities or particles from the CNT-PVA solution. Centrifugation at 4000 RPM for 30 min was done several times unless the solution becomes clear and no CNT left in solution. Thirdly, to remove excess PVA from PVA-CNT solution, filter paper Anodisc 47 (Whatman) with the pore size 200 nm and diameter 47 mm is used. Filtered CNT-PVA are then collected and dried under vacuum.

Finally, CNT-PVA solution is sonicated in an ultrasonic bath for 6 h to uniformly disperse in solution. After attachment of carboxylic group, MWCNTs were

investigated by Fourier Transform Infrared spectroscopy (FTIR). **Figure 2** shows the FTIR spectrum of PVA treated MWCNTs in which peaks appears at 3425 and 1390 cm^{-1} are identified with O-H bond bending and stretching. The frequency associated with these vibrations is due to hydrogen bonding linked with functional groups. The peak observed at 1260 cm^{-1} is due to C–O bond stretching vibrations in phenol and alcohol. Another peak appeared at 1663 cm^{-1} is due to C=O stretching of functional group (COOH) considered at the surface of MWCNTs. In addition, C–H stretch vibrations correspond to 2856 and 2924 cm^{-1} band. Thus, FTIR is a powerful tool to see the chemical changes in the carbon system. MWCNTs are attached to the tungsten tips not only to increase the spatial resolution but also to increase the aspect ratio as well. According the literature survey, many groups have used CNTs as a scanning probe. Some of them used direct grown of CNT on cantilever or by picking the single CNT using special system installed within the SEM.

However, these instruments are costly or require special techniques to attach single MWCNT on AFM probe. Here, we have used dielectrophoresis method which is not only the cost-effective process but also a time saving and a simple process to attach the CNT. To attach the single MWCNTs on chemically etched tungsten probe, sharpness of the tip, applied frequency and diameter of the tip are the key parameters. One electrode is the etched tungsten wire while other is gold ring electrode. Using micropipette small droplet of functionalized MWCNTs is dropped into the gold ring electrode and with the help of micro-manipulator, the tip is brought closer to MWCNTs solution droplet and form a meniscus which cover only the edge part of etched tungsten tip. Using this technique, possibility to attach the CNT at the edge is increased. Otherwise, CNTs may attach at the surface of tungsten tip. Alternating voltages (6 volts at 2.2 MHz) were applied to the electrodes causes to generate the electric filed and CNTs were began to align parallel and eventually attached to the sharp edge of tungsten tip. However, at this stage MWCNT cannot be used for scanning purpose because CNT is attached with tungsten probe using Van der Waals and not sufficient to hold it during scanning. The homemade 3D AFM setup along with all electronics components is shown in **Figure A2**.

2.3 MWCNTs welding and cutting using FIB

We have utilized a focused beam of gallium ions (FIB) to align and attach the CNT on tungsten tip. The FIB system used (QUNTA 3D FEG) is a dual beam type

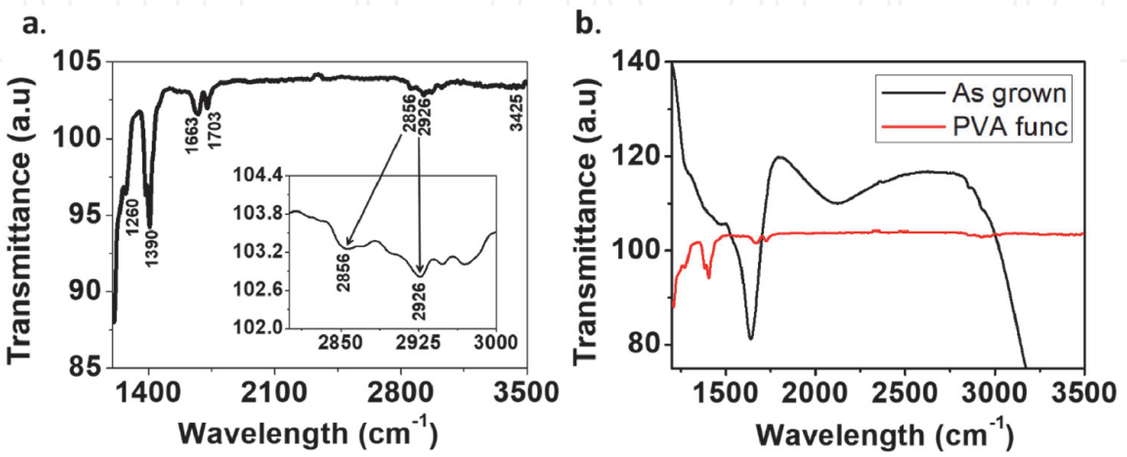

Figure 2.
Functionalization of MWCNT. (a) FTIR spectra depicts attachment of functional groups in CNTs: Peaks reveal 1200–3500 confirm the presence of functional group in purified CNTs. Inset image clearly shows the peaks at 2856 and 2926. (b) Comparison between the PVA-functionalized and as grown MWCNT.

where the electron and ion column are placed vertically (at 0°) and at an angle 52°, respectively. Alternatively, the same viewing angle of another gun can be obtained by tilting the sample back and forth by 52°.

Using the FIB process, CNT can be welded and shorten to use for AFM scanning. Our Fabrication of MWCNT based AFM probe comprises of four steps. Firstly, using electron beam induced deposition (EBID) hydrocarbon, CNT is welded on the etched part of tungsten tip (**Figure 3(b)**). The carbon atoms are deposited at the interface of tungsten which makes the CNT to attach firmly with tungsten. Secondly, CNT is aligned in the FIB system through the ion beam bending (IBB) [27] (**Figure 3(c)**). FIB is irradiated from the top. In the complete process of CNT alignment, acceleration voltage was set to 30 kV, resolution was 512 pixels × 442 pixels and FIB image magnification was 5000. Beam current as well as acceleration voltages can be increased to reduce the alignment time, however, should be optimized to avoid sample damage. We have used this method on 110–170, 50–80 and 20 nm CNT and it has been found that exposure time (for alignment process) to MWCNT is directly proportion to the diameter of MWCNT. For example, MWCNT with the diameter 20 nm takes less exposure time as compared to 50–80 or 110–170 nm MWCNT. The variables that affect the alignment process includes FIB magnification, exposure time, beam current and accelerating voltage. To produce good welding, many combinations can be made that produce good results. On the

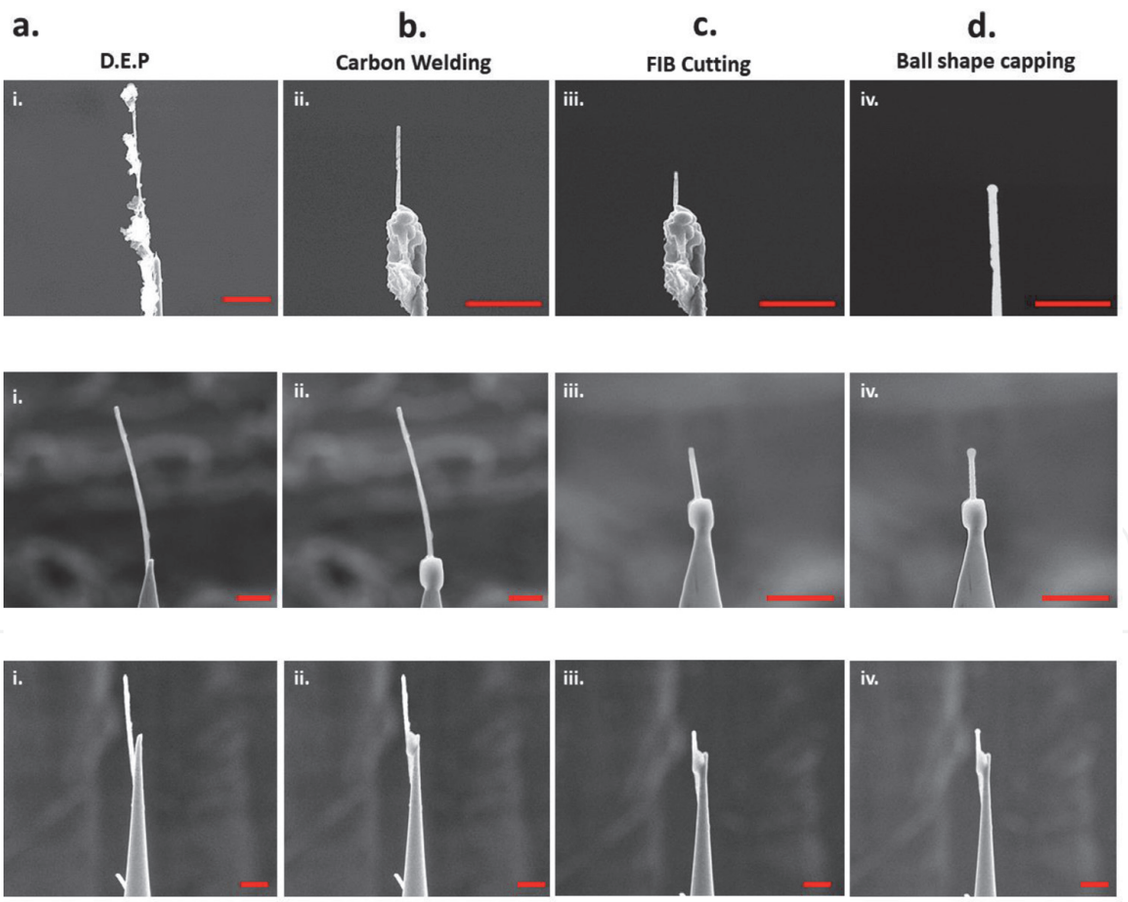

Figure 3.
Fabrication of MWCNT AFM probe. (a) As attached using DEP, some impurities are also attached with MWCNT which can be removed using lower current ion beam. (b) After hydrocarbon deposition (welding) on the interface of MWCNT and Tungsten probe. (c) Alignment of MWCNT using IBB process (d) using gallium ion bombardment extra length of CNT is cut off. To give some offset from the sidewall (in case of AAO sample or samples having vertical side walls), ball shape (using hydrocarbon) was deposited on the top of MWCNT. Diameter of MWCNT is 20, 60 and 120 nm. Scale bar is 1 μm.

other hand, all these parameters are carefully chosen while considering the CNT diameter under investigation, length and initial orientation. Thirdly, gallium ions are used to shorten the CNT (**Figure 3(c)**). After the selection of suitable length of CNT, i.e. we choose 300, 500, 700 nm and 1μm length, extra length was cut-off using gallium ions (**Figure 3(d)**). **Figure 3** shows the welding, alignment, cutting and ball shape capping of CNT on tungsten probe.

After that, the tip is shorten to less than 0.5 mm and attached to one end of quartz tuning fork (QTF) using the Torr Seal®. Quality factor, Q, of 45,000±500 in air was routinely obtained. Q factor of TF should be as higher as possible to obtain the highest sensitivity and resonance frequency, f, was shifted from 32,768 Hz to 32,310 Hz. QTF was excited at 15 mV which corresponds to 2.85 nm free oscillation amplitude.

3. Results and discussion

Herein, we have validated the working of the algorithm to measure the 3D profile of different samples (AAO and silicon pillars). Proposed algorithm enjoys all the advantages of conventional AFM. In addition to this, it has the capability to the measure the high aspect ratio features present above or below the sample. Here, we have used AAO sample to measure the internal morphology of the holes and 3D scanning of silicon pillars. To measure the internal morphology of the hole, firstly, the raster scan is performed using the MWCNTs based AFM probe: MWCNTs probe is attached using the FIB process on the Tungsten (W) apex which is further attached with the one prong of quartz tuning fork. Once raster scan is completed, feedback loop is turned off to start the 3D scanning of the hole. Positions of the holes and protrusion can be clearly seen from the raster scan image. Secondly, the algorithm is executed to scan the internal topography of via hole. Proposed algorithm can be summed up in four steps: Finding the location of hole(s), moving the tip to the bottom of the hole to be scanned internally, finding the first sidewall along the lateral direction, making the motion corresponding to the sidewall detected.

3.1 Finding the location of holes

Location of the hole can be founded in various ways. One of the easiest ways is do the raster scan over certain area at high resolution. However, due to the high aspect ratio of the AAO holes, the tip wear might occur which is not suitable to do the 3D scanning of the hole. For 3D scanning of the hole, the tip should have perfect symmetry so that the accurate imaging can be done inside of the hole. Other method is to do the force-distance curve or mapping, amplitude-distance curves or mapping over a certain area i.e. doing the amplitude-distance curve at each pixel and recording the coordinates and Z position. Lowest Z scanner value can be marked by red color and highest value with blue. Each individual pixel locally quantifies physical properties and interactions. By this, lot of information (elasticity, adhesion) can be mapped directly of the sample internal topography. In the **Figure 4**, we have done the mapping of certain area of AAO in which location of the can be clearly seen with different color contrast. In **Figure 4(i)**, FD curve is done on solid surface which has sharp change at 450 nm and on contrary side, **Figure 4(ii)** has rapid decrease in amplitude at 201 nm which shows which shows the tip can penetrate up to 249 nm. However, at this stage, tip is restricted not to go beyond the set point level. Later on, once the location of the hole is determined, tip can be pushed deep inside to measure the exact depth of the hole.

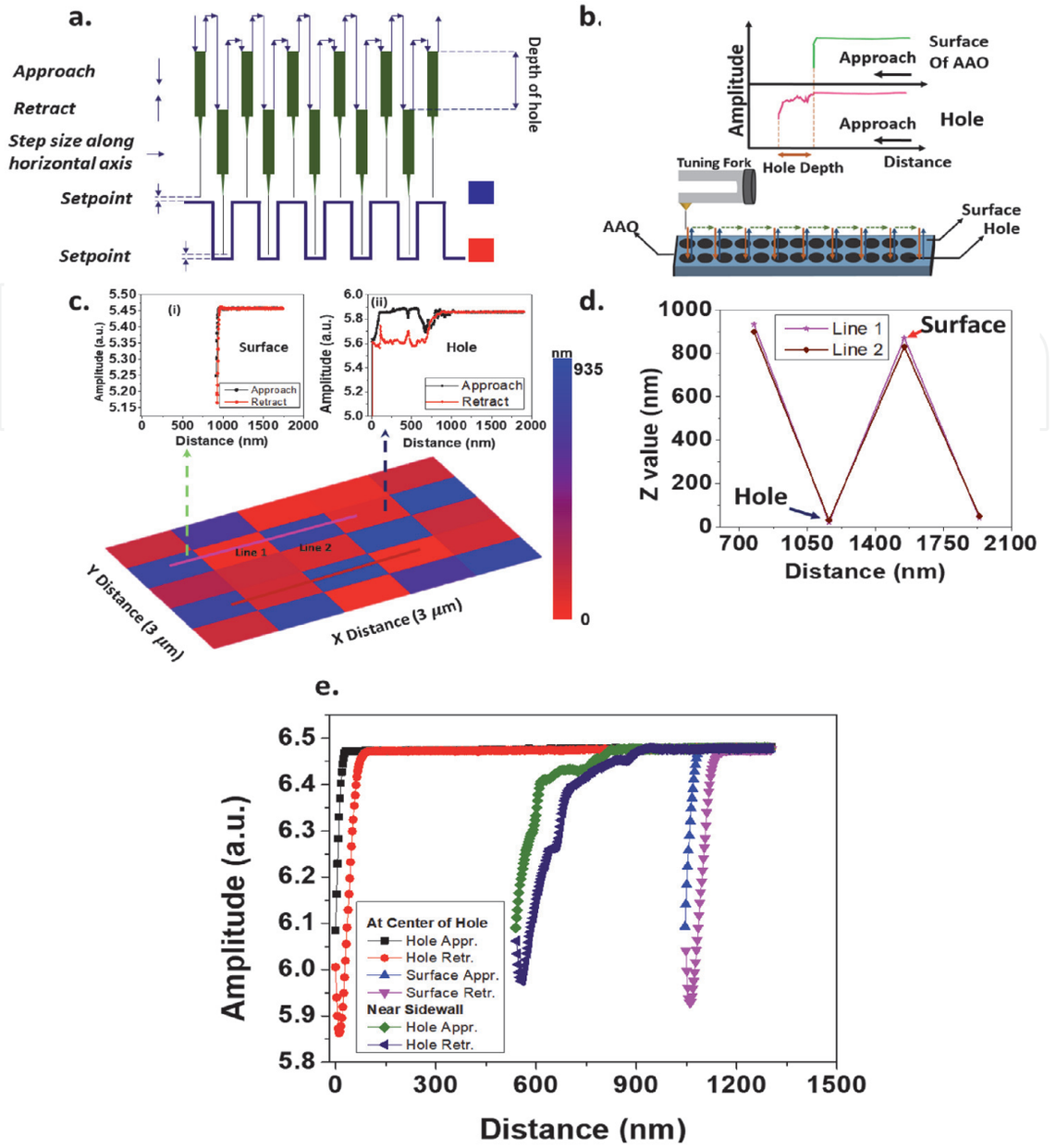

Figure 4.
Finding the location of holes by mapping. (a) FD mapping scheme in which the highest Z scanner value (surface or protrusion) is marked by blue color and lowest scanner value (hole) is marked by red color. (b) Using QTF, followed by MWCNT and tungsten probe, amplitude-displacement curve was measured at different position of AAO sample. Rapid decrease in amplitude (without wrinkle-top graph in green) shows the surface and amplitude-distance measurement with wrinkles shows the location of hole (lower graph in pink). Difference in both points (where the probe touches the surface and bottom) gives the depth of hole. (c) Mapping was done using 20 nm MWCNT on AAO surface over 3 micron area. From the graph (i) and (ii), it is clear that when Amplitude-displacement curve done on surface it does not have any hump while measured on hole, it shows some humps which corresponds to the Van der Waals interaction of probe with the inner sidewall of hole. CNT goes 935 nm gives the depth of the hole (d) Line 1 and line 2 shows the hole profile or depth profile of hole. From this data depth of the hole can be estimated which is 480 nm (Sample AAO – Actual depth—500 nm as purchased). (e) FD curve taken at surface, at the centre of hole, near the side wall of AAO hole.

3.2 Finding the bottom and depth measurement of via hole

First, for scanning the internal topography of the hole, one can click at the center of the hole and scanner will move at the center of the hole. Algorithm is designed in such a way that mouse click will bring the scanner to the required coordinates (at the center of the hole). Then the tip will move along $-Z$ axis to reach to the bottom of the hole. If the hole is not uniform, then the possibility still exist that the tip might not touch to the bottom due to the many local minima present inside. As the

tip pierces in to the hole, amplitudes remains constant. However, if the tip is not at the center or non-uniform hole, then it might experience van der Waals interaction between MWCNT and sidewall of AAO sample as shown in **Figures 4(c)—(ii)** and **5**. Zongwei et al. [28] have used the DVD surface for force curve measurement at the pit edge as well as on plane surface and they have found that the ripple and wavelike wrinkles can be easily occurred if the FD measurement was done at the pit's edge. However, this van der Waals forces might restrict the tip to reach at the bottom. To resolve this, the FD is measured away from the sidewalls so that van der Waals are less likely to appear when the tip is at the center of the hole as shown in **Figure 4(e)**.

Once can interpret the interaction of MWCNT to the sidewall by observing the FD curve profile as shown in **Figure 5**. At some point, amplitude tends to decrease due to interaction of AFM probe with sidewalls. As the interaction dominates the setpoint, i.e., amplitude decreased more than the setpoint, tip is retracted. **Figure 4** shows a good method to find the exact location of the hole. However, to measure the actual depth of the hole, this is not the point where the tip has to stop. We try to push the tip inside of the hole by tracking the amplitude change and it has been found that when the amplitude drops more than 60%, then we can say that it might be the bottom of the hole or in worst case the tip has been stuck to the hole. However, this problem can be overcome by measuring the FD curve in near surrounding of hole and recording the XY-coordinates with scanner value. Coordinate with the lowest scanner value might be bottom of the hole. After that, the scanner will move to that coordinate having minimum $-Z$ value corresponds to the minimum position of the hole. We have used the AAO sample with pore diameter 350 nm and different depth (300 nm, 500 nm, 1 μm with tolerance±5%). FD curve is performed on different which gives the real depth of the sample. With 120 nm sample, depth of 1st AAO sample was measured 915 nm, 485 and 285 nm for second sample which corresponds to the vendor supplied values. In addition to this, we have done FD curves at the same position many times to check the reproducibility of the data as well as tip wear was less likely to found (Appendix). More than 10 times FD curves are performed and the difference between the first and final

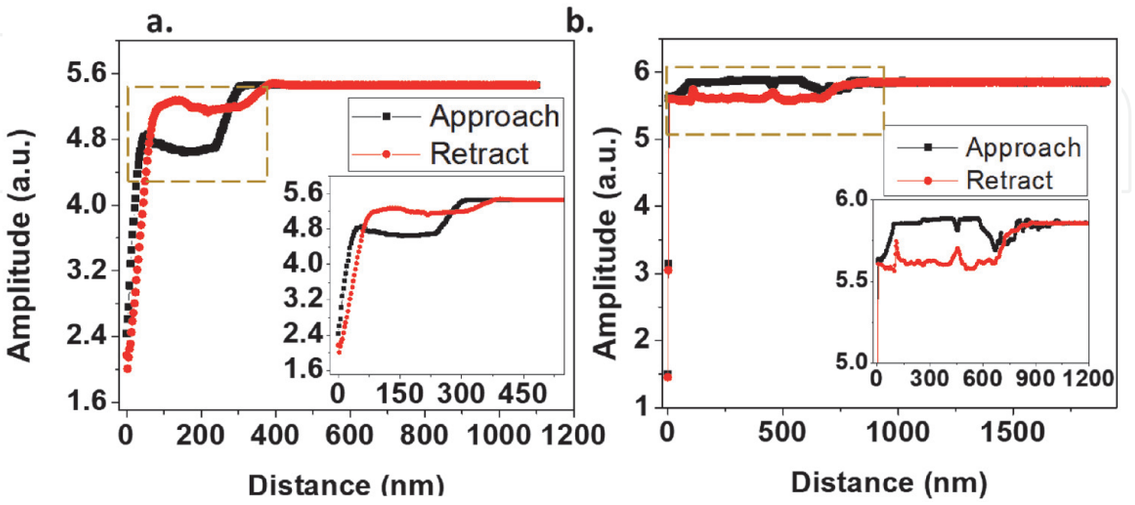

Figure 5.
MWCNT interaction with sidewall of via holes. (a) Amplitude-displacement curve was performed on AAO sample with depth 300 nm with pore diameter 350 nm. In 300 nm sample, first drop in amplitude shows that the tip entered in to the hole and it might experience the sidewall or AD curve is done near the sidewall. As tip moves towards the bottom of the hole, at some point, rapid drop in amplitude occurs which shows the tip touched to the bottom. (b) FD curve on AAO sample with depth 1 μm *and pore diameter was 350 nm. The depth was scanned approximately 930 nm. In both case, 120 nm MWCNT was used.*

depth was only 10 nm. However, the Van der Waals forces may vary measurement-to-measurement as the tip goes deep inside the hole. Moreover, there was no significant damage to the apex of the tip. In **Figure 5(c)**, 120 nm shows the best result in stability as well as depth measurement and 3D scanning of deep holes. On the contrary side, 20 nm is suitable for 3D scanning of shallow holes as well as protrusion.

3.3 Finding the first sidewall of hole

As tip find the real bottom of the hole, it will start moving in either direction (along +X axis) to find the first sidewall. Starting from the center (bottom) of the hole, tip start piercing the direction of sidewall by moving forward and backward along all the axis individually as shown in **Figure 6**. At each step, either the sidewall is present or not, its location is stored in variable. This is important because at some point the tip might not found the sidewall, then the direction of motion of probe will be decided by 'location of previous sidewall' and it can only be done storing the direction of sidewall at each step. In addition to this, if the tip has lost the sidewall (due to drift), then tip will move to the nearest sidewall present by tracking the history of motion that probe has moved.

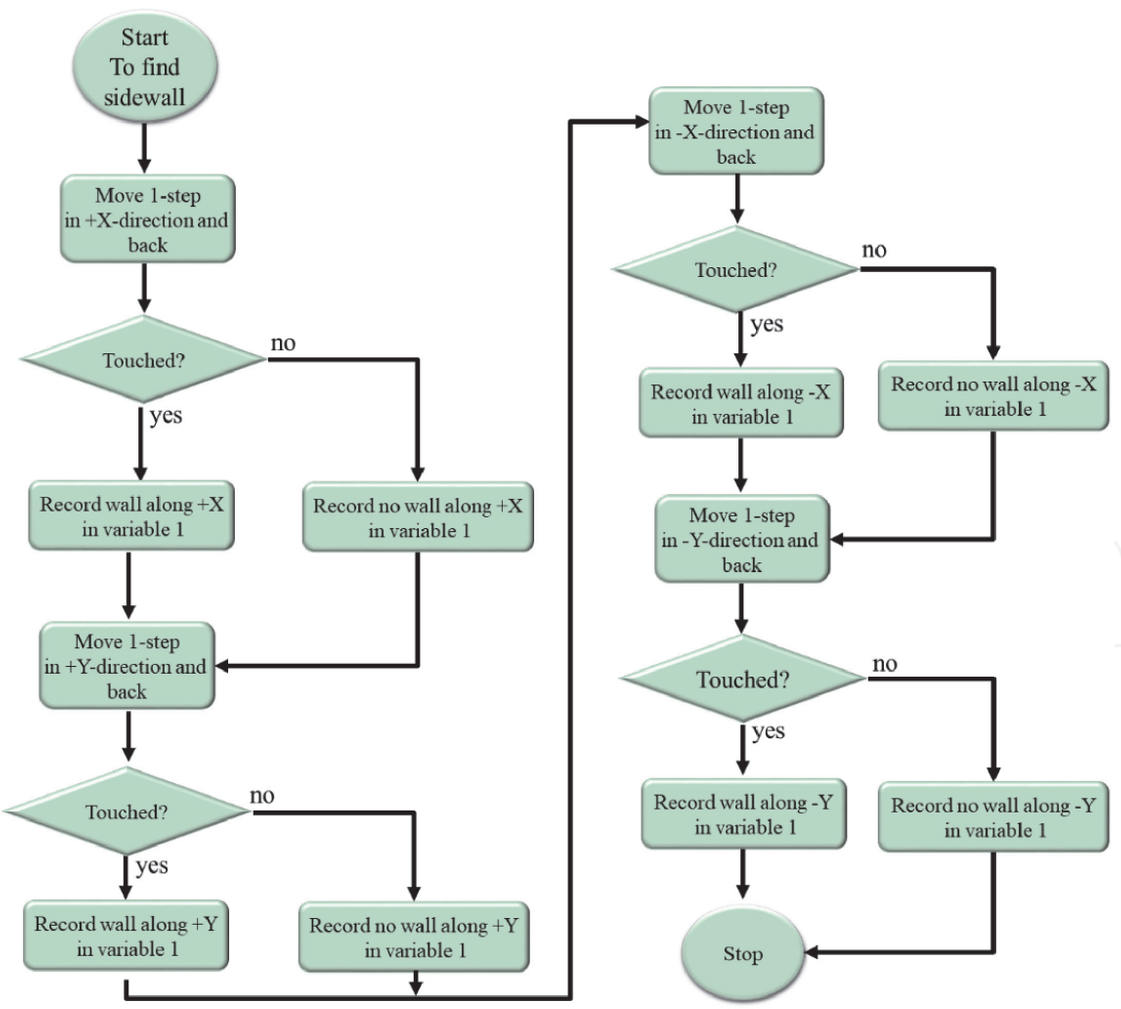

Figure 6.
Algorithm to find the direction of sidewall. As the tip reaches at the bottom of the hole, it starts to find the sidewall in all direction by moving forward-backward motion and tracking the amplitude. Any encounter with the sidewall causes to decrease in amplitude. Direction of the sidewall is stored in the variable1 to make the movement accordingly.

For example, tip move one step in +X direction and move back by tracking the amplitude. If the amplitude remains the same, it means there is no sidewall along +X direction. Similarly, the same phenomena is repeated by scanner for other axes (+Y, −X, −Y). The direction of sidewall is checked at every step. If the sidewall is detected in any direction, the corresponding motion will be performed by the scanner (Appendix).

3.4 Making the motion corresponding to the sidewall detected

As the tip is scanning to find the sidewall along all the direction, at some point, the sidewall will be detected along +X axis and according the algorithm the tip will move along +Y direction. After that, the direction of sidewall will be checked again. If the sidewall is along +Y direction, then the motion will be along -X axis. Similarly, following the counterclockwise scheme, motion will be along +X direction if the sidewall will be in -X direction. If at next step, tip found no sidewall then the scanner will move in the direction where the last sidewall was. This technique helps the tip to strictly follow the boundary of the hole and with the motion decided by the algorithm, the perfect boundary of the feature can be determined sophisticatedly. The situation is more interesting when the tip experience two or three sidewalls and motion of the scanner will be followed as described in **Table A1** (Appendix). However, if all sidewall direction is found then tip is assumed to be trapped and should be retracted along +Z direction for its safety. **Figure 6** shows the working strategy to find the side wall of algorithm to track the boundary of the hole and tracking the amplitude as shown in **Figure 7**. To know the exact shape of the boundary, X and Y step size can be varied. However, there are two types of steps, i.e., jump step and motion step. The first one is jump step along any axis to check the direction of sidewall, which is usually greater than the motion step size. This is necessary to make the tip at a safe distance so that the tip not wear or to minimize the van der Waals forces between the tip and the sidewall. The motion step can be decreased to few nanometers for high resolution and to measure the exact shape of feature. After that, arithmetic is done by the algorithm, by considering the jump step, to calculate the diameter of each complete rim scan by adding the jump step to diameter obtained from 3D scanning.

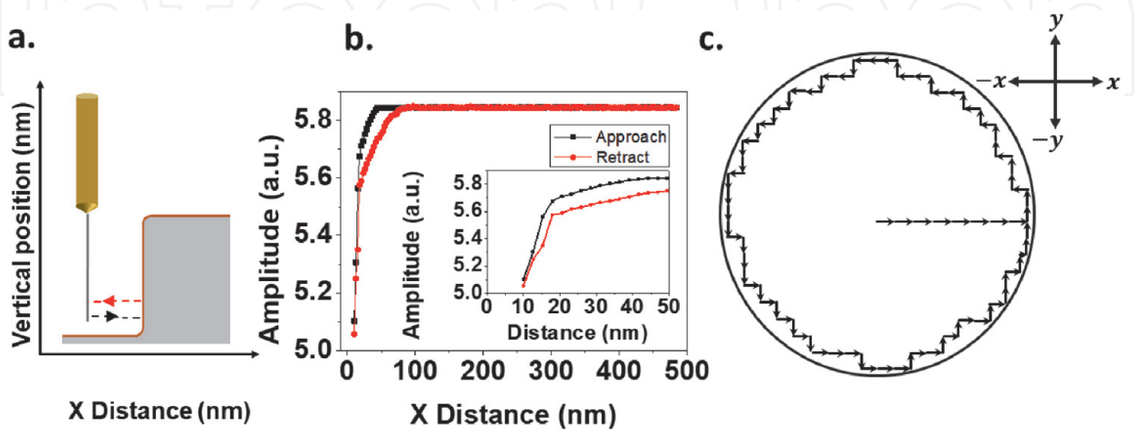

Figure 7.
Working strategy of Algorithm to find the sidewall and scan the via holes. (a) Algorithm record the amplitude before and after moving towards the position of sidewall. If there is sidewall, rapid decrease in amplitude is detected as can be seen in (b). (c) Motion of the tip to follow the boundary of the via hole. The step size can be varied for high resolution. Tip start from the centre of the hole and start moving along +X direction to find sidewall. As it finds the sidewall, it starts following the boundary of hole in xy plane in counter clockwise.

3.5 3D scanning of hole AAO

To test the feasibility of the proposed three-dimensional imaging algorithm of via holes as well as protrusion, we first done the simulation in the LABVIEW software (Appendix). The versatility of the software can be seen in such a way that any irregular shape of hole as well as protrusion can imaged using this algorithm.

The above-mentioned algorithm is implemented in LabVIEW software and tested on Anodic Aluminum Oxide (AAO) sample bought from Vida Biotechnology CO. LTD. We have three samples with 300 nm, 500 nm and 1 μm depth. Diameter of the holes were 350 nm. For protrusion, silicon pillars bought from NT-MDT having the approx. Height of 500 nm and 3 μm periodicity along lateral and 2.1 μm along diagonal direction. Dimension of the sample was as: 2.5 × 2.5.

Figure 8(b) shows the 3D image of AAO hole having the depth of 650 nm when the algorithm is applied to scan the internal topography of hole. Z step is set to 34 nm, however for higher resolution it can be decreased. Moreover, **Figure 8(c)** is the AFM image obtained using conventional AFM which cannot go deep more than 530 nm due to low aspect ratio. This shows our 3D AFM algorithm has strong potential to scan the features having high aspect ratio. As the tip goes deep inside the hole more than a micron, Van der Waals forces between the tip and sidewall also increases which may lead to the instability of the CNT. However, this problem can be overcome by using increasing number of layers of CNT so that it will be rigid, less flexible and stable for 3D scanning.

As the location of the holes (coordinates) is evident from the FD mapping (Z scanning) as shown in **Figure 4(c)**, next holes can be easily scanned. For example,

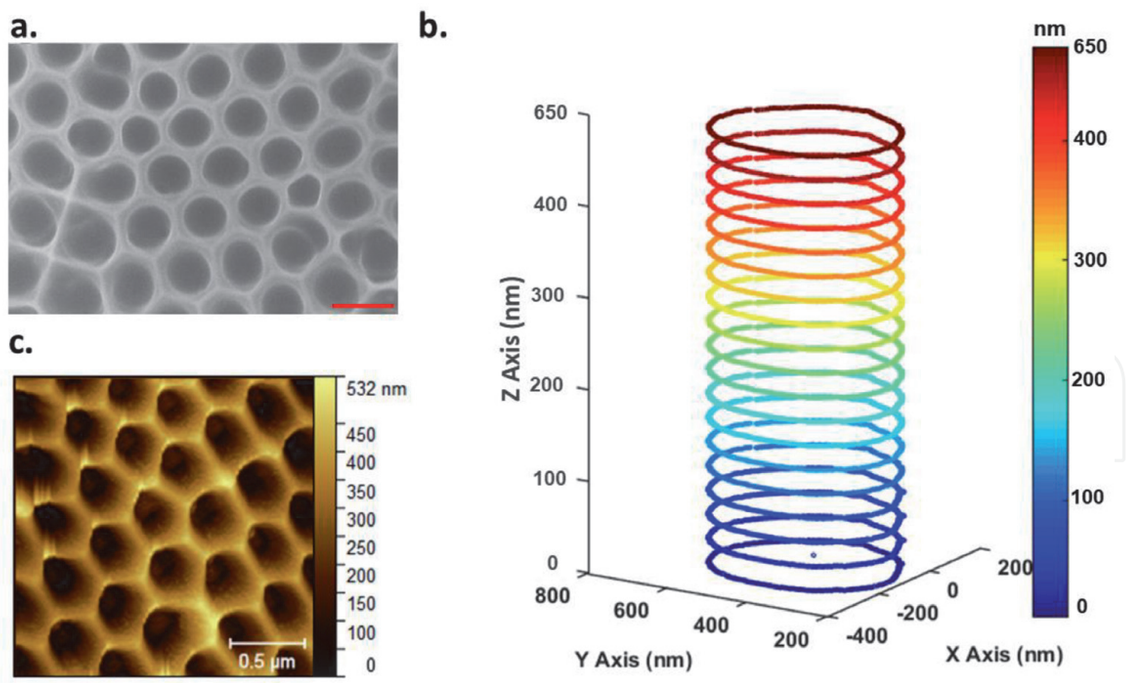

Figure 8.
AAO image with the depth 1um and pore diameter 350 nm. (a) SEM image of AAO. (b) 3D image of inside of hole which shows that the tip scanned 650 nm depth. Tip goes deep inside of hole and find the bottom where it has to start the 3D scanning as marked by the dot in figure. Then it moves in either direction (+X) to find the sidewall. Once the sidewall is found, tip start to follow the boundary. After completing the one rotation (360°), scanner retracted along +Z direction to start new rim scan. When the straight line is found during scanning, it means that the tip is escaped from the hole or tip finished scanning the hole (straight line not shown in figure). (c) Raster image obtained from conventional AFM used to find the location of hole. Due to the low aspect ratio of the conventional AFM, it cannot go deep and limited to 532 nm, however, the original sample depth is 1 μm. Scale bar is 500 nm.

once the 3D scan of first hole is completed and tip is escaped from the hole (in line profile straight line shows that the tip is escaped from the hole), using the coordinates of next hole, tip moves along –Z direction and reaches at the bottom of the hole. Once it touches to the bottom, 3D scanning is done in the same fashion as of first hole.

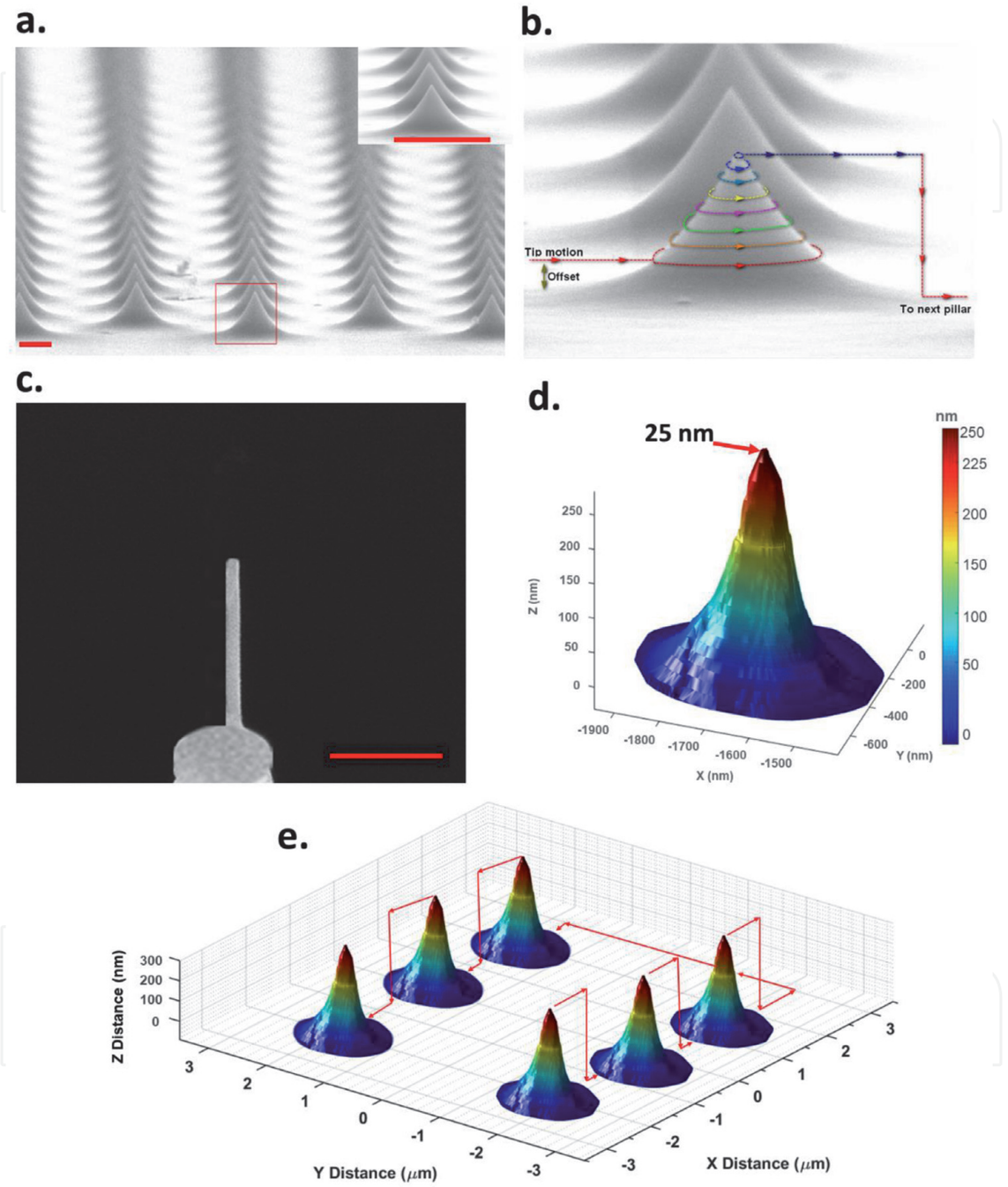

Figure 9.
Image of silicon pillars. (a) SEM image of silicon pillars. (b) Lines showing the scan direction of tip. As the tip comes near the surface it is retracted (offset) few hundreds of nm to avoid any interface of surface with the tip. As the tip is moving in +X direction to find the sidewall, at some point it find the sidewall of silicon pillar and according to algorithm, it start to find the boundary of the pillar. As once rotation completed, tip retracted along +Z direction to scan next rim. If the straight line is found in the scan, as shown in figure, it means that the tip has completed scanning the pillar and similarly next pillar can be scanned using the same scheme. (c) FIB treated 20 nm MWCNT (without capping) used to obtain the 3D profile of silicon pillar (d) 3D image of silicon pillar obtained from the 3D scanning algorithm with the step size 19 nm along X, Y direction and 20 nm along +Z direction. However, the step size along all axis can be even smaller for high resolution. The scale bar is 500 nm. The edge of the tip is limited to the radius of the probe. In our case, tip radius of arc grown CNT is 20 nm. (e) 3D image of silicon pillars: After completing one pillar, tip is brought near to the surface again (moved along –Z direction) to scan the next pillar. Motion of the probe is shown by the red arrow in figure.

In addition to this, algorithm is applied to obtain the 3D topography of the silicon pillars. Tip start to scan the pillar in either direction. Once it encounter the sidewall of pillar, it start to follow the boundary of the silicon pillar and on completion of one rotation, scanner retracted along +Z direction to complete the next rim scan. The process continuous unless it complete scanning the pillar. Resolution of 3D image depends upon the thickness of AFM probe. We have used 20 nm tip to scan the pillar which means the last (top edge) rim scan should be approximately equals to the diameter of the CNT as shown in **Figure 9**.

In addition to this, as the tip completes once pillar, the tip can be pushed deliberately near to the surface and moved in +X direction to find the second pillar and so on.

4. Conclusion

MWCNT tips are one of the best candidates to further investigate different materials in AFM imaging world, enhancing tip lifetime, eliminating the artifacts and increasing the resolution by decreasing the tip-surface forces. Many algorithms has already been proposed and implemented to scan the deep trenches, sidewall roughness and to measure other 3D parameters. However, none of them can able to 3D scan the deep via holes, which has the vertical sidewalls and real time 3D imaging protrusions features like silicon pillars. As TSVs have potential application in NAND flash memories, 3D meteorology, and 3D system integration. So, exact location of via holes, depth and internal roughness of sidewall should be measured accurately. In this work we have proposed an algorithm which has ability to scan the features above and below the surface such as TSV and silicon pillars. We have tested the algorithm on AAO in which location of holes, depth of holes as well as internal roughness of sidewalls are measured. In addition to this, real time 3D scanning has been performed by the algorithm on silicon pillars (protrusion) and it has been found that it is a best choice to measure the features having high aspect ratio. We believe that impact of this algorithm will not be limited to only the semiconductor field. In general, getting the 3D topography is a crucial issue for measuring the parameters like surface roughness, hole depth and locations etc. So far, several algorithms has been proposed which employs special type of probes, but these are specially designed to measure the structures like trenches as discussed earlier. The new method described here is a unique since it can image any kind of feature (present above or below the surface).

A. Appendix

A.1 Functionalization of MWCNT

To functionalize the MWCNTs, 1 g of PVA was completely dissolved in 60 ml of water at room temperature. After that, 0.2 mg of MWCNTs was added into the above-mentioned solution and mixture was stirred at 70°C for 4–12 h. A centrifugal separator was used to remove the impurities or particles from the CNT-PVA solution. Centrifugation at 4000 RPM for 30 min was done several times unless the solution becomes clear and no agglomerated CNTs left in solution. To remove excess PVA from PVA-CNT solution, filter paper (Anodisc 47, Whatman) with the pore size 200 nm and diameter 47 mm was used. Filtered CNTs-PVA are then

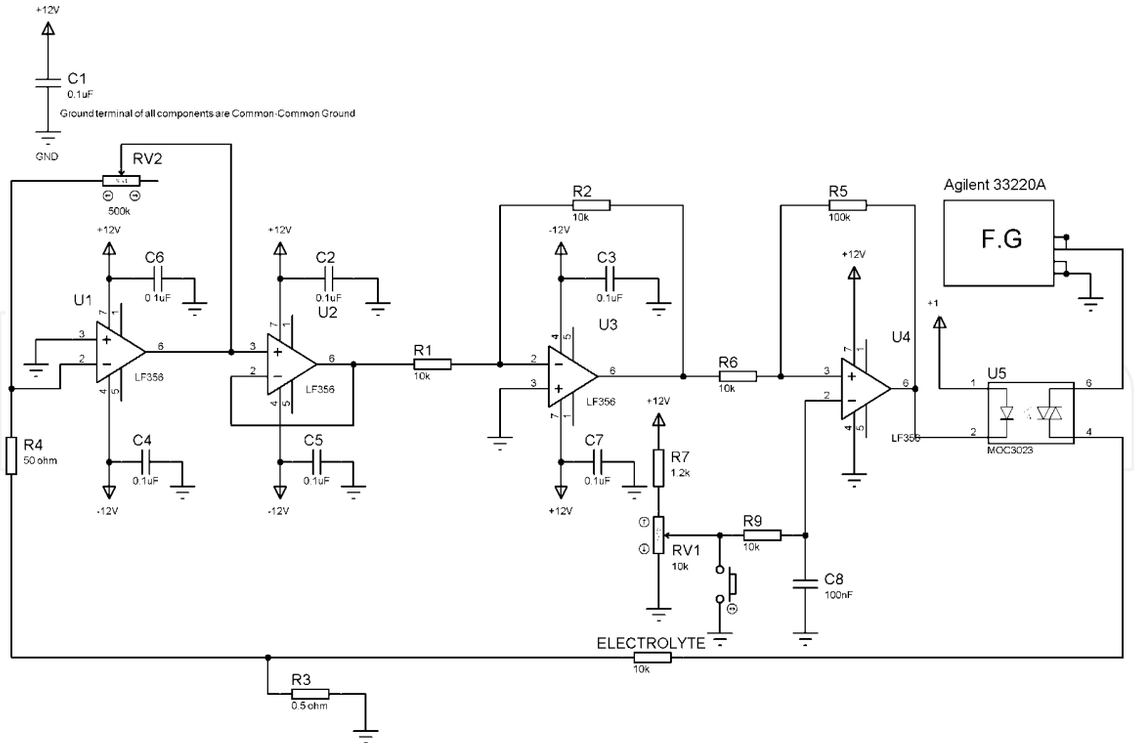

Figure A1.
Automatic shutoff circuit for electrochemical etching of tungsten wire. Etching circuit is divided in to two resistors, i.e., 0.5 and 50 Ω (Connected to real and virtual ground, i.e., input to the current amplifier). Second stage amplifier is a voltage follower which makes the signal stable during the etching. Third stage amplifier is an inverting amplifier which inverts the signal from the first stage so that it can be compared to the set point. At the very last moment of etching, when lower part of the tip is about the drop, there might be some fluctuation in the signal and tip can be blunt or uniformity of the tip can be disturbed. To avoid this, Schmitt trigger is used at the comparator which makes the signal stable at the last moment of etching. Solid state relay is used to reduce the shut-off time. This automatic cut-off circuit has the shut-off time 0.5 μs.

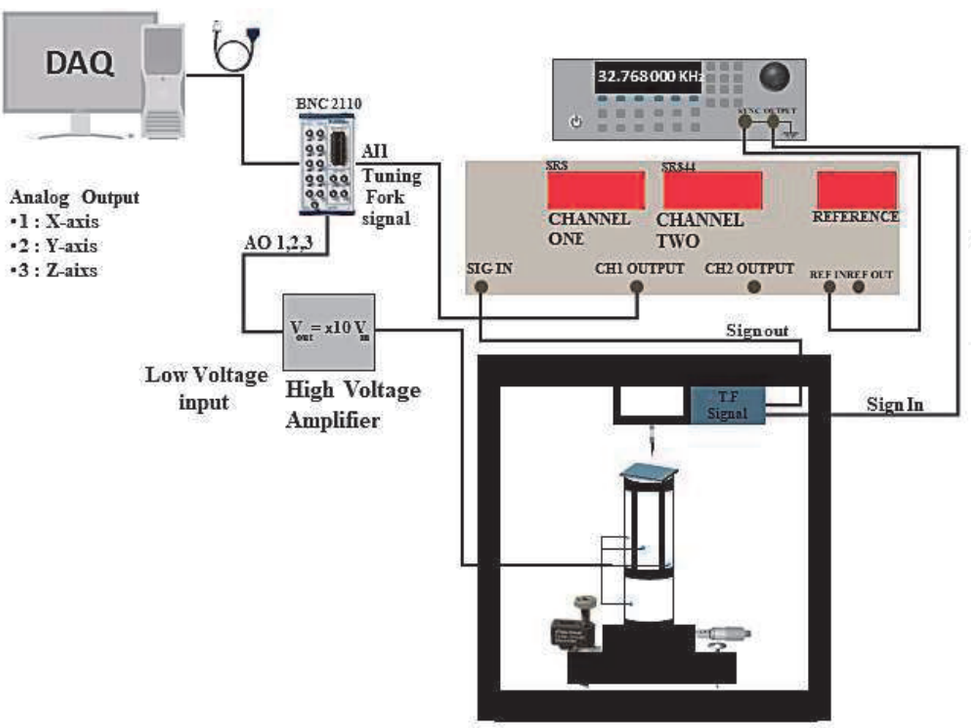

Figure A2.
Homemade setup for 3D AFM, composed of tuning fork sensor, lock-in amplifier, PC based digital controller, and a tube scanner.

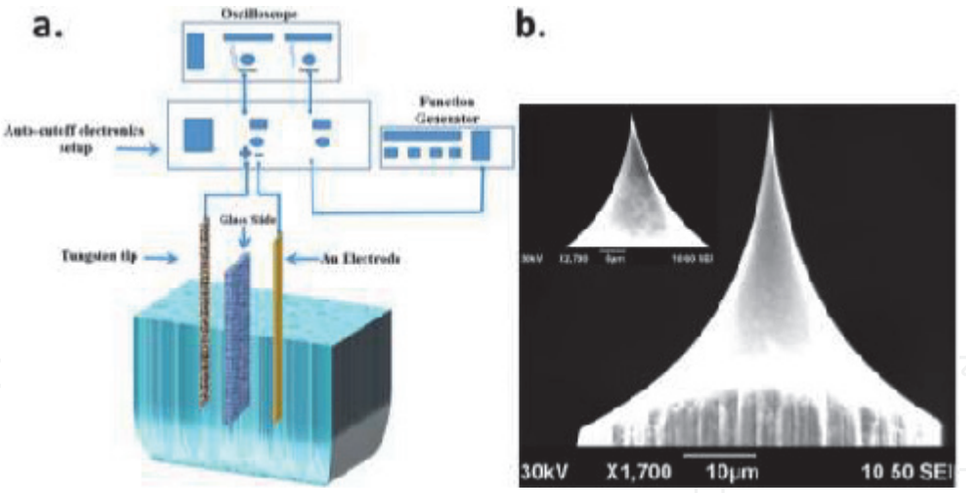

Figure A3.
Experimental setup for tungsten wire etching. (a) Gold wire is used as anode and tungsten wire acts as cathode. As the etching begins, bubbles travel from anode to cathode which may deform the meniscus shape. A glass slide is placed between the electrodes to avoid this problem. (b) SEM image of tungsten wire after it has been etched using KOH solution. Once the wire has been etched, it is washed with hot D.I water to reduce the oxide layer around the etched part. We have used 2 M concentration of KOH solution. Etching takes approximately 70 s to complete the etching. After etching 5–6 tips, the solution needs to be replaced. Otherwise, etched shape may be not uniform or the surface of the tungsten becomes rough. Almost all of tips are produced uniformly and the average tip radius is found to be 80 nm.

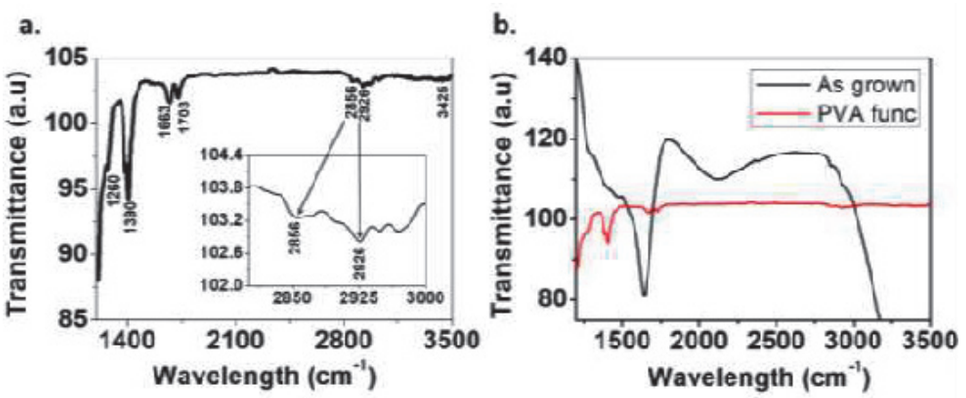

Figure A4.
FTIR spectra for functionalized MWCNT. (a) FTIR spectrum depicts attachment of functional groups in CNTs: Peaks in the range of 1200–3500 confirm the presence of functional group in purified CNTs. Inset image clearly shows the peaks at 2856 and 2926. (b) Comparison between the PVA-functionalized and as grown MWCNT.

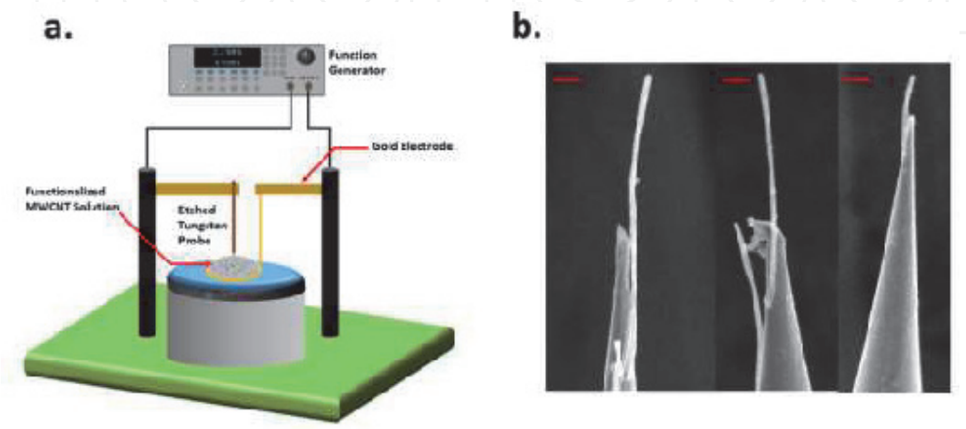

Figure A5.
Dielectrophoresis setup for attachment of multiwall carbon nanotube on chemically etched tungsten probe. (a) Function generator is used to apply AC voltage which generates electric field and consequently attracts the CNT towards the tungsten probe. (b) SEM image shows a single MWCNT attached to the tungsten probe via van der Waals forces. Scale bar is 500 nm.

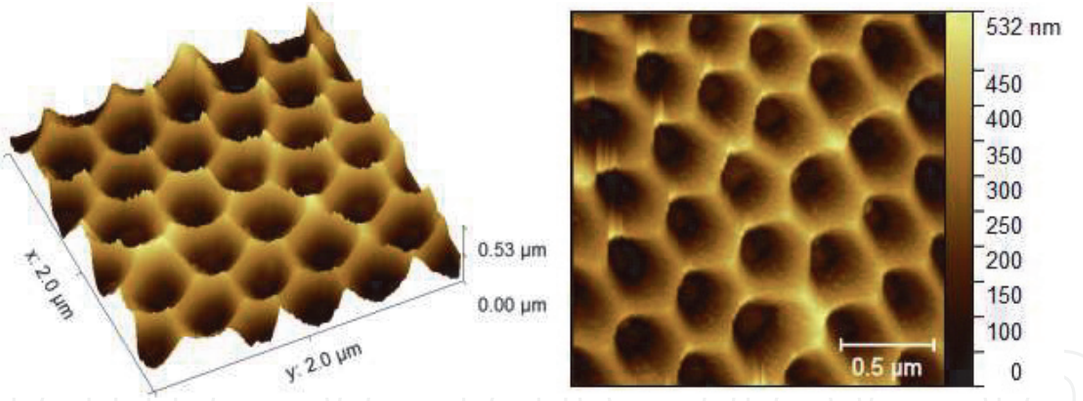

Figure A6.
AFM image of AAO sample obtained from home built AFM using the MWCNT. Raster scan mode was applied to find the location of holes.

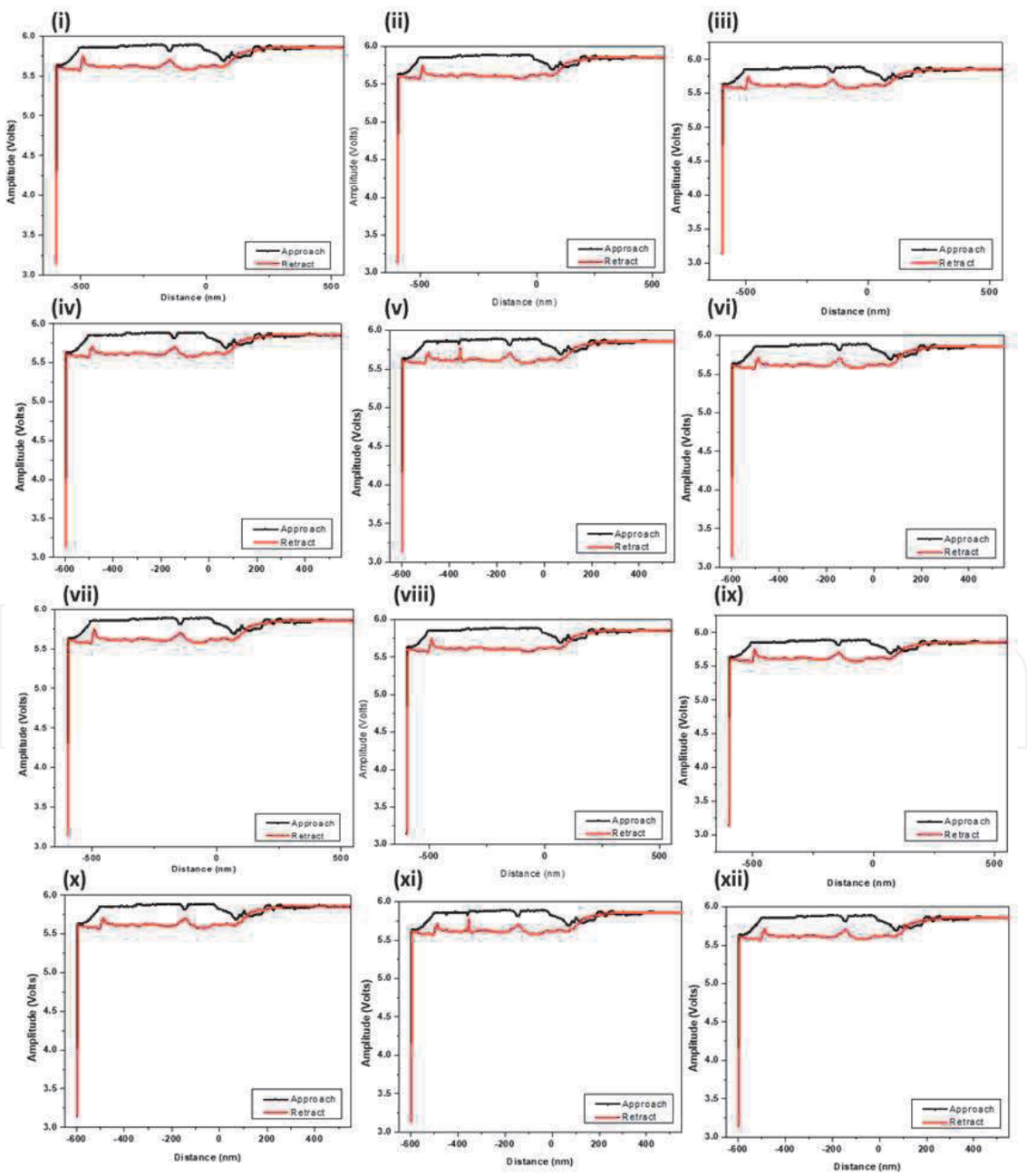

Figure A7.
FD curves were measured at the different holes in AAO sample having the depth of 1 µm. Sharp decreases imply that the tip touches to the bottom of the hole, and the depths are estimated as ~935 nm similar from all data.

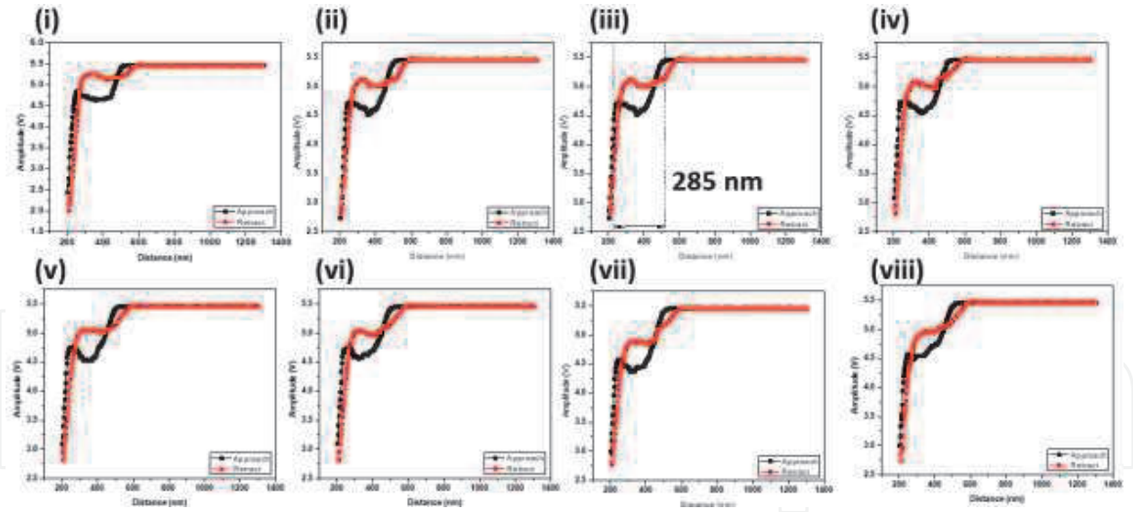

Figure A8.
FD curves are measured at different holes on AAO sample having the depth of ~300 nm. Measured data show that the depth is approximately 285 nm. Sharp increases indicate that the tip touches to the bottom of the hole.

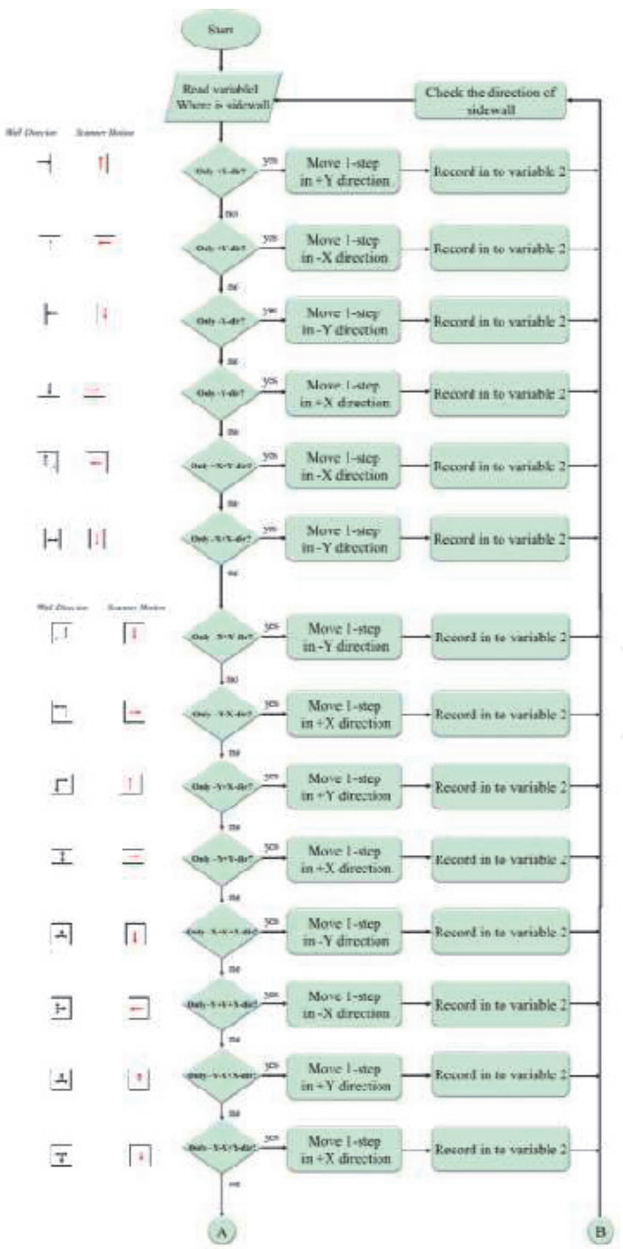

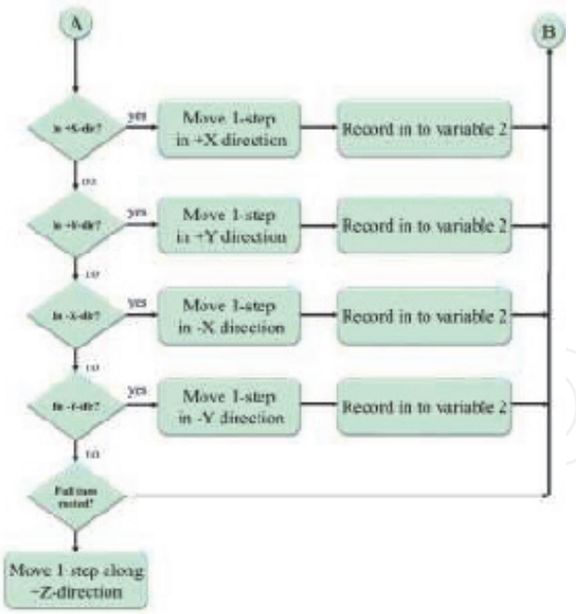

Figure A9.
After the wall is encountered by the probe by tracking the difference in amplitude, motion of the scanner is determined according to ***Table A1****. However, if the probe is unable to find the sidewall, it will move along the direction where the previous sidewall was. This gives the appropriate correction of the sidewall direction to follow the exact shape of the boundary. By this strategy, any shape of either hole or protrusion is scanned perfectly.*

S.#	Sidewall direction				Scanner motion
	+X	+Y	−X	−Y	
1	—	—	—	—	Previous direction of sidewall
2	—	—	—	SW	Along +X
3	—	—	SW	—	Along −Y
4	—	—	SW	SW	Along +X
5	—	SW	—	—	Along −X
6	—	SW	—	SW	Along −X
7	—	SW	SW	—	Along −Y
8	—	SW	SW	SW	Along +X
9	SW	—	—	—	Along +Y
10	SW	—	—	SW	Along +Y
11	SW	—	SW	—	Along −Y
12	SW	—	SW	SW	Along +Y
13	SW	SW	—	—	Along −Y
14	SW	SW	—	SW	Along −X
15	SW	SW	SW	—	Along −Y
16	SW	SW	SW	SW	Along +Z

SW: sidewall detected, "—": not detected.

Table A1.

collected and dried under vacuum. Finally, CNT-PVA was dissolved into DI water and the solution is sonicated in an ultrasonic bath for 6 h to uniformly disperse in solution. After attachment of carboxylic group, MWCNTs were investigated by Fourier transform Infrared spectroscopy (FTIR), as shown in **Figure A4**. The peaks observed at 1390 and 3425 cm^{-1} are identified with O–H bond bending and stretching, respectively [29]. The peaks observed at 1260 and 1663 cm^{-1} are due to C–O and C=O stretching of functional groups, respectively [29]. In addition, C–H stretching vibrations correspond to 2856 and 2924 cm^{-1} peaks [30].

A.2 Attachment of MWCNT by dielectrophoresis

MWCNTs are attached to the tungsten tips not only to increase the spatial resolution but also to increase the aspect ratio as well. To attach the single MWCNT on chemically etched tungsten probe, sharpness of the tip, applied frequency, and field intensity are the key parameters. One electrode is the etched tungsten wire,

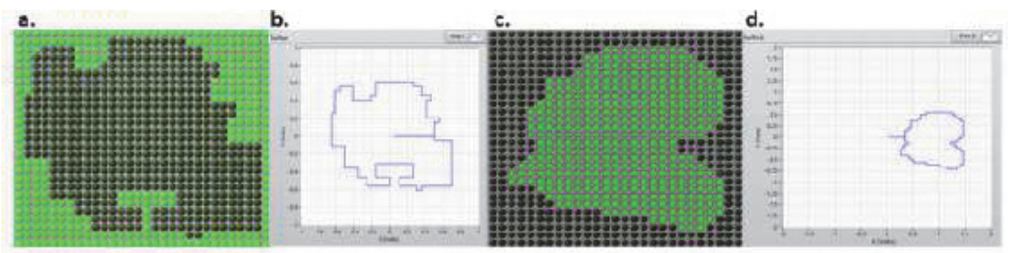

Figure A10.
Simulation results of the algorithm for complicated hole and protrusion. (a) A random shape hole was drawn to check the versatility of the algorithm, where dark portion indicates the empty hole. (b) Line profile shows a simulation result of the tip trance. The tip starts scanning from the centre and move in along +X axis direction to find the side wall. Once the sidewall is detected, tip start to follow the boundary of the hole. Afterwards, one complete rotation is completed. (c) A random shape protrusion was drawn, where green portion represents the protrusion. (d) The simulation result of scanning shows a line profile of protrusion. Working methodology to scan the protrusion is the same as the hole.

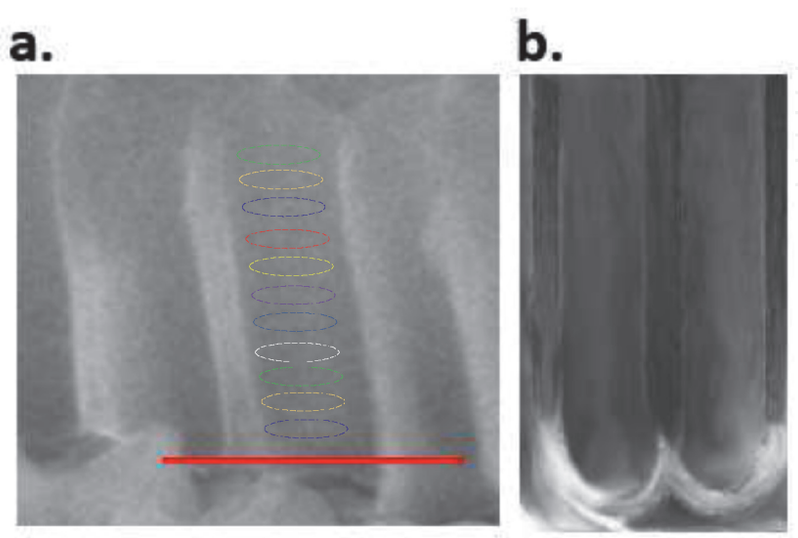

Figure A11.
Cross section views of fractured AAO samples (a) in the middle part (b) near the bottom. Circles show the expected 3D scanning traces. Tip starts scanning from the bottom and raised a step along +Z direction as one rotation completed. Scale bar is 1 μm.

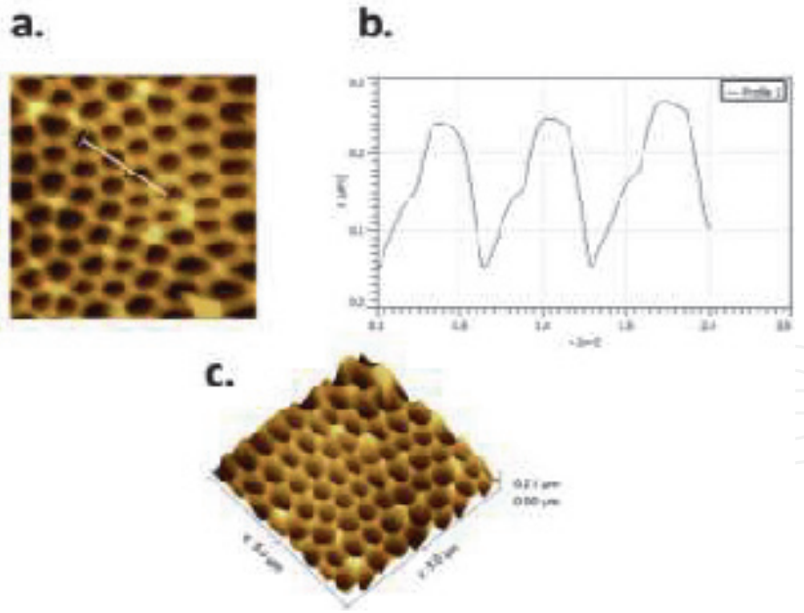

Figure A12.
Raster scan image of AAO sample using commercially available AFM with silicon cantilever. (a) Raster scan image with silicon cantilever showing that the AFM probe cannot go beyond 210 nm. (b) Line profile of the hole showing the depth of the hole is only 100 nm. However, original sample has depth around 1 μm. (c) 3D view of AAO sample.

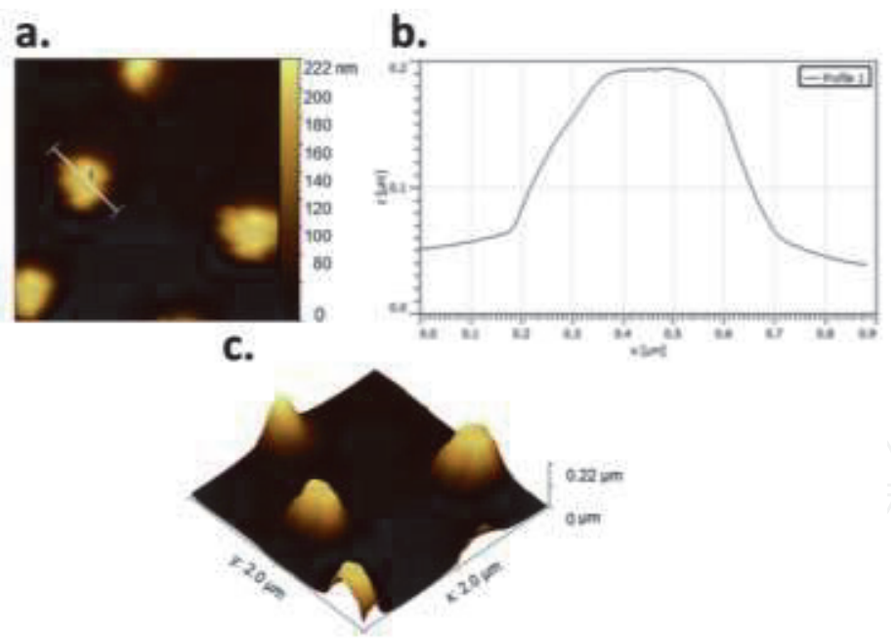

Figure A13.
Raster scan image of silicon pillars using commercially available AFM using silicon cantilever. (a) Raster scan image with silicon cantilever showing that the AFM probe cannot go beyond 222 nm due to low aspect ratio. (b) Line profile of the silicon pillar which shows the height of one pillar is 120 nm as well as broad peak unlike the real sample. However, original sample has height around 500 nm*. (c) 3D view of silicon pillars.*

while other electrode is a gold ring. AC voltages (6 V at 2.2 MHz) are applied to the electrodes, and CNTs are attached to the sharp edge of the tungsten tip. At this stage, van der Waals forces hold the CNTs, which are not strong enough to be used for scanning purpose.

Author details

Imtisal Akhtar*, Malik Abdul Rehman and Yongho Seo
Department of Nanotechnology and Advanced Materials Engineering, Sejong University, Seoul, South Korea

*Address all correspondence to: writetoimtisal@hotmail.com

References

[1] Benkart P, Kaiser A, Munding A, Bschorr M, Pfleiderer HJ, Kohn E, et al. 3D chip stack technology using through-chip interconnects. IEEE Design and Test of Computers. 21 November 2005; **22**(6):512–518

[2] Topol AW, La Tulipe DC, Shi L, Frank DJ, Bernstein K, Steen SE, et al. Three-dimensional integrated circuits. IBM Journal of Research and Development. July 2006;**50**(4.5):491–506

[3] Cho S-J, Ahn BW, Kim J, Lee JM, Hua Y, Yoo YK, et al. Three-dimensional imaging of undercut and sidewall structures by atomic force microscopy. Review of Scientific Instruments. 24 February 2011;**82**(2): 023707

[4] Miyashita H, Kanada H, Ogawa T. Three dimensional shape measurement of via-holes for the production of multi-layers circuit boards. Journal of The Japan Institute of Electronics Packaging. 1 July 2004;**7**(4):333–338

[5] Akhtar I, Rehman MA, Choi W, Kumar S, Lee N, Cho SJ, et al. Three-dimensional atomic force microscopy for ultra-high-aspect-ratio imaging. Applied Surface Science. 1 March 2019; **469**:582-592

[6] Nakamura M, Kitada H, Sakuyama S. Direct depth measurement tool of high aspect ratio via-hole for three-dimensional stacked devices. Journal of Surface Analysis. 2014;**20**(3): 182–186

[7] Fischer AC, Forsberg F, Lapisa M, Bleiker SJ, Stemme G, Roxhed N, et al. Integrating MEMS and ICs. Microsystems & Nanoengineering. 28 May 2015;**1**:1-6

[8] Wood J. The top ten advances in materials science. Materials Today. 2008;**11**:40–45

[9] Kim D, Sahin O. Imaging and three-dimensional reconstruction of chemical groups inside a protein complex using atomic force microscopy. Nature Nanotechnology. 2015;**10**:264–269

[10] Dufrêne YF et al. Imaging modes of atomic force microscopy for application in molecular and cell biology. Nature Nanotechnology. 2017;**12**:295–307

[11] Dai H, Hafner JH, Rinzler AG, Colbert DT, Smalley RE. Nanotubes as nanoprobes in scanning probe microscopy. Nature. 1996;**384**:147–150

[12] Wiesendanger R, Mulvey T. Scanning probe microscopy and spectroscopy. Measurement Science and Technology. 1995;**6**:600

[13] Wilson NR, Macpherson JV. Carbon nanotube tips for atomic force microscopy. Nature Nanotechnology. 2009;**4**:483–491

[14] Astrova E, Fedulova G, Zharova YA, Gushchina E. Side-wall roughness of deep trenches in 1D and 2D periodic silicon structures fabricated by photoelectrochemical etching. Physica Status Solidi C. 2011;**8**:1936–1940

[15] Hua Y, Buenviaje-Coggins C, Lee YH, Lee JM, Ryang KD, Park SI. New three-dimensional AFM for CD measurement and sidewall characterization. In: Metrology, Inspection, and Process Control for Microlithography XXV. Vol. 7971. International Society for Optics and Photonics. 20 April 2011. p. 797118

[16] Dai G, Wolff H, Pohlenz F, Danzebrink H-U, Wilkening G. Atomic force probe for sidewall scanning of nano-and microstructures. Applied Physics Letters. 2006;**88**:171908

[17] Ku Y-S, Huang KC, Hsu W. Characterization of high density

through silicon vias with spectral reflectometry. Optics Express. 2011;**19**: 5993–6006

[18] Jin J, Kim JW, Kang C-S, Kim J-A, Lee S. Precision depth measurement of through silicon vias (TSVs) on 3D semiconductor packaging process. Optics Express. 2012;**20**:5011–5016

[19] Lee JS et al. Multifunctional hydrogel nano-probes for atomic force microscopy. Nature Communications. 2016;**7**:11566

[20] Gu JM, Hong SJ. In: 2015 IEEE Electrical Design of Advanced Packaging and Systems Symposium (EDAPS). IEEE; 2015. pp. 27-30

[21] Orji NG et al. Tip characterization method using multi-feature characterizer for CD-AFM. Ultramicroscopy. 2016;**162**:25–34

[22] Liu H-C et al. Proceedings of SPIE: 69222J

[23] Choi J et al. Evaluation of carbon nanotube probes in critical dimension atomic force microscopes. Journal of Micro/Nanolithography, MEMS and MOEMS. 2016;**15**:034005

[24] Kneedler R et al. Proceedings of SPIE:905–910

[25] Seo Y, Park J-Y, Kim K, Lee N. General algorithm and method for scanning a via hole by using critical-dimension atomic force microscopy. Journal of the Korean Physical Society. 2014;**64**:1643–1647

[26] Kulakov M, Luzinov I, Kornev K. Capillary and surface effects in the formation of nanosharp tungsten tips by electropolishing. Langmuir. 2009;**25**: 4462–4468

[27] Park BC, Jung KY, Song WY, Ahn SJ. Bending of a carbon nanotube in vacuum using a focused ion beam. Advanced Materials. 2006;**18**:95–98

[28] Xu Z, Fang F, Dong S. Electronic Properties of Carbon Nanotubes. Rijeka, Croatia: InTech; 2011

[29] Kim UJ, Furtado CA, Liu XM, Chen GG, Eklund PC. Raman and IR spectroscopy of chemically processed single-walled carbon nanotubes. Journal of the American Chemical Society. 2005;**127**(44):15437–15445

[30] Kazmi SJ, Shehzad MA, Mehmood S, Yasar M, Naeem A, Bhatti AS. Effect of varied Ag nanoparticles functionalized CNTs on its anti-bacterial activity against *E. coli*. Sensors and Actuators, A: Physical. 2014;**216**:287–294